Biophysical Chemistry, 38 (1990) 99–109
Elsevier

BIOCHE 01502

Influence of end-to-end diffusion on intramolecular energy transfer as observed by frequency-domain fluorometry

Joseph R. Lakowicz [a], Wieslaw Wiczk [a], Ignacy Gryczynski [a], Henryk Szmacinski [a] and Michael L. Johnson [b]

[a] *University of Maryland, School of Medicine, Center for Fluorescence Spectroscopy, Department of Biological Chemistry, 660 West Redwood Street, Baltimore, MD 21201 and* [b] *University of Virginia, Department of Pharmacology, Charlottesville, VA 22908, U.S.A.*

Received 2 January 1990
Revised manuscript received 16 April 1990
Accepted 17 April 1990

Energy transfer; Diffusion; Distance distribution; Frequency-domain fluorometry; Fluorescence spectroscopy; Molecular dynamics

We investigated the influence of end-to-end diffusion on intramolecular energy transfer between a naphthalene donor and dansyl acceptor linked by polymethylene chain. A range of viscosities from 0.6 to 200 cP were obtained using propylene glycol at different temperatures (0–80 °C) and methanol at 20 °C. The intensity decays of naphthalene were measured in the frequency domain. Several theoretical models, including distance distributions, were used to fit the data. The results indicate that end-to-end diffusion of flexible donor-acceptor pairs can be detected and quantified using frequency-domain fluorometry, even in the presence of a distribution of donor-to-acceptor distances.

1. Introduction

The phenomenon of nonradiative resonance energy transfer (RET) has been widely used for determination of intramolecular distances and distance distributions in bichromophoric systems [1–4] and labeled macromolecules [5–10]. In the case of a single donor (D)-to-acceptor (A) distance, without diffusion, there is a single time-invariant rate of energy transfer, resulting in relatively simple decay kinetics for the donor. In flexible D-A pairs there exists a distribution of D-to-A distances, which in turn results in complex donor decay kinetics [3,9,10]. The time-dependent energy transfer becomes still more complicated if conformational fluctuations occur during the excited-state lifetime of the donor. Generally, in a fluid solution, the mean diffusion distance $\Delta\bar{x}$ during the lifetime of the donor $\bar{\tau}$ is given by

$$\Delta\bar{x} = (2D\bar{\tau})^{1/2}, \tag{1a}$$

$$D = kT/6\pi\eta R \tag{1b}$$

Diffusion coefficients (D) may be estimated by the Stokes-Einstein relationship (eq. 1b), where k is Boltzmann's constant, η the viscosity and R the molecular radius. During the last three decades the influence of diffusion on energy transfer has been treated theoretically by several authors [11–16]. Some of these treatments are developed from Förster kinetics and diffusion theory (Stern-Volmer kinetics) [14]. Particularly, the influence of diffusion on intramolecular energy transfer has

Correspondence address: J.R. Lakowicz, University of Maryland, School of Medicine, Center for Fluorescence Spectroscopy, Department of Biological Chemistry, 660 West Redwood Street, Baltimore, MD 21201, U.S.A.

Abbreviations: A, acceptor; D, donor; NMN, nonanoyl-1-methylnaphthylamide; NU2D, dansylundecanoylundecanoyl-1-methylnaphthylamide; PG, propylene glycol; MeOH, methanol; RET, resonance energy transfer.

NMN

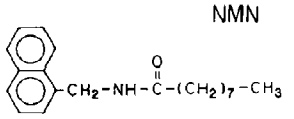

NU2D

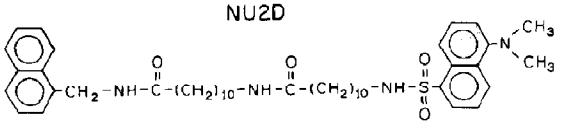

Scheme 1.

been investigated by Haas and co-workers [17,18]. Recently, in a simulation study, Beechem and Haas [19] discussed difficulties and possibilities to recover both distance distributions and segmental diffusion from time-resolved fluorescence measurements. At present there exists a lack of accurate time-resolved measurements of energy transfer in the presence of end-to-end diffusion. In this paper, we present frequency-domain measurements of diffusion-dependent energy transfer between naphthalene and dansyl connected by a polymethylene chain (NU2D) (scheme 1). The experimental data have been analyzed using different theoretical models.

2. Theory

There are several theoretical analytical expressions to describe the donor decay kinetics in the presence of multiple randomly distributed acceptors, with and without translational diffusion [15,16,20]. We reasoned that energy transfer will occur dominantly to the nearest acceptor, so that these theories may be applicable to our D-A pairs, which contain a single acceptor. Furthermore, the temperature (diffusion) dependence of the recovered diffusion coefficients should reveal the effects of viscosity, even if only by the trends in the recovered values. At this time we are not able to analyze the data in terms of end-to-end diffusion of a single D-A pair due to the lack of a theoretical framework and appropriate software.

2.1. Förster kinetics without diffusion

In the presence of randomly distributed acceptors, the donor fluorescence decays nonexponentially according to

$$I_D(t) = I_D^0 \exp\left\{ -\frac{t}{\tau_D^0} - 2\gamma\left(\frac{t}{\tau_D^0}\right)^{1/2} \right\} \tag{2}$$

where τ_D^0 denotes the donor fluorescence decay time in the absence of energy transfer, $\gamma = C_A/C_A^0$, and C_A represents the molar concentration of the acceptor [20]. C_A^0 is the molar critical concentration of acceptor,

$$C_A^0 = \frac{3000}{2\pi^{3/2} N R_0^3} \tag{3}$$

In this expression, N is Avogadro's number and R_0 the critical transfer distance given by Förster

$$R_0^6 = \frac{9000(\ln 10)\kappa^2 \phi_D^0}{128\pi^5 N n^4} \int_0^\infty F_D(\lambda)\epsilon_A(\lambda)\lambda^4 \, d\lambda \tag{4}$$

where κ^2 is the orientation factor, ϕ_D^0 the quantum yield of the donor in the absence of acceptor, n the refractive index, N Avogadro's number, $F_D(\lambda)$ the emission spectrum of the donor with the area normalized to unity, $\epsilon_A(\lambda)$ the absorption spectrum of the acceptor in units of M^{-1} cm^{-1}, and λ the wavelength in nm. If the molecular orientations are random, due to Brownian rotation, then $\kappa^2 = 2/3$. In our analysis, using eq. 2, C_A will be the floating parameter. The influence of end-to-end diffusion should increase the amount of energy transfer and thus result in increasing apparent values of C_A.

2.2. Förster kinetics with diffusion

We selected two models to analyze the energy-transfer data in terms of diffusion; namely, those of Yokota and Tanimoto [15] and Gosele et al. [16]. Yokota and Tanimoto [15] used the Padé approximate method to determine an expression for Förster energy transfer in a fluid medium. They obtained an approximate expression for the

donor fluorescence decay in the presence of diffusing acceptors,

$$I_D(t) = I_D^0 \exp\left\{ -\frac{t}{\tau_D^0} - 2\beta\gamma\left(\frac{t}{\tau_D^0}\right)^{1/2} \right\} \quad (5)$$

The parameter β is given by

$$\beta = \left(\frac{1 + 10.87x + 15.5x^2}{1 + 8.743x} \right)^{3/4} \quad (6)$$

where

$$x = D\alpha^{-1/3}t^{2/3}, \qquad \alpha = R_0^6/\tau_D^0 \quad (7)$$

Gosele et al. have improved eq. 5 for the long-time behavior [16] and obtained a modified value of β

$$\beta = \left(\frac{1 + 5.47 + 4x^2}{1 + 3.34x} \right)^{3/4} \quad (8)$$

In our fitting procedure, D and C_A will be floating parameters.

2.3. Distance distribution model without diffusion

We also analyzed the fluorescence data in terms of distance distributions. In this case the model is for a single acceptor near each donor, but the model does not account for D-to-A diffusion. Assume the decay of the donor ($I_D(t)$) in the absence of energy transfer is a single exponential

$$I_D(t) = I_D^0 \exp\left[-\frac{t}{\tau_D^0} \right] \quad (9)$$

where τ_D^0 is the decay time of the donor. Consider a single D-A pair in which the acceptor is present at a unique distance r. The donor decay of this molecule with a unique D-A distance is given by

$$I_{DA}(r,t) = I_D^0 \exp\left[-t/\tau_D^0 - k_{DA}t \right] = I_D^0 \exp\left[-\frac{t}{\tau_{DA}} \right] \quad (10)$$

The rate of energy transfer is given by

$$k_{DA} = \frac{1}{\tau_D^0}\left(\frac{R_0}{r}\right)^6 \quad (11)$$

with R_0 being the Förster distance. When an acceptor is present at a single distance the donor decay remains a single exponential.

The intensity decay of the donor becomes more complex if the acceptor is located over a range of D-A distances, as is expected for our flexible D-A pairs. Since each individual D-A pair is characterized by a specific distance r, the intensity decay of each donor is still a single exponential and is given by

$$I_{DA}(r,t) = I_D^0 \exp\left[-\frac{t}{\tau_D^0} - \frac{t}{\tau_D^0}\left(\frac{R_0}{r}\right)^6 \right]. \quad (12)$$

However, the observed decay contains contributions from D-A pairs at all accessible distances, and is thus more complex than a single exponential. The intensity decay of the ensemble of D-A pairs is given by the average of the individual decays weighted by the distance probability distribution ($P(r)$) of the D-A pairs

$$I_{DA}(t) = I_D^0 \int_0^\infty P(r) \exp\left[-\frac{t}{\tau_D^0} - \frac{t}{\tau_D^0}\left(\frac{R_0}{r}\right)^6 \right] dr \quad (13)$$

In this report we assume that the probability distribution is a Gaussian

$$P(r) = \frac{1}{\sigma\sqrt{2\pi}} \exp\left[-\frac{1}{2}\left(\frac{r - \bar{r}}{\sigma}\right)^2 \right] \quad (14)$$

where $\bar{r}$ is the average, and σ the standard deviation of the distribution. We report the widths of the distributions in terms of the half-widths (hw, full-width at half-maximum), which is related to σ by hw = 2.354σ. We note that the Gaussian may not be the theoretically correct form for the distance distribution. However, we found that this model was adequate to account for the data. It should be noted that eq. 14 is appropriate for distributions in which the D-A distances are static during the donor decay.

At this time we are not able to fit our data simultaneously to the distance distribution and to the diffusion coefficient. The presence of diffusion will be monitored by changes in the apparent mean distance ($\bar{r}$) and apparent half-widths (hw) of the distributions. The observation of these changes and correlations between distribution

parameters and mean diffusion distances ($\Delta\bar{x}$) will be the subject of our data analysis and interpretation.

2.4. Frequency-domain expression

The intensity decays of the donor emission were measured using the frequency-domain method [21–23]. The experimental values are the phase (ϕ_ω) and modulation (m_ω) of the emission over a range of modulation frequencies (ω). Irrespective of the form of the decay, the frequency response can be predicted for any $I(t)$ using

$$N_\omega = \frac{\int_0^\infty I(t) \sin \omega t \, dt}{\int_0^\infty I(t) \, dt} \tag{15}$$

$$D_\omega = \frac{\int_0^\infty I(t) \cos \omega t \, dt}{\int_0^\infty I(t) \, dt} \tag{16}$$

The calculated (c) phase and modulation values for the assumed decay law are given by

$$\phi_{c\omega} = \arctan\left[\frac{N_\omega}{D_\omega}\right] \tag{17}$$

$$m_{c\omega} = \left[N_\omega^2 + D_\omega^2\right]^{1/2} \tag{18}$$

It is informative to analyze the frequency responses of the donor controls and the D-A pairs using the multiexponential model,

$$I(t) = \sum_i \alpha_i \exp[-t/\tau_i] \tag{19}$$

where α_i are the pre-exponential factors and τ_i the associated decay times. The fractional contribution of each component is given by $f_i = \alpha_i\tau_i/\sum_j \alpha_j\tau_j$. The parametized form of the donor-alone decay time is needed for calculation of the distance distributions [9,10]. Additionally, the multiexponential analysis of the D-A pair donor decays reveals the extent of heterogeneity due to the D-A distance distribution. For the multiexponential model the transforms can be represented analytically [24]

$$N_\omega = \frac{1}{J}\sum_i \frac{\alpha_i \omega \tau_i^2}{1 + \omega^2\tau_i^2} \tag{20}$$

$$D_\omega = \frac{1}{J}\sum_i \frac{\alpha_i \tau_i}{1 + \omega^2\tau_i^2} \tag{21}$$

where the normalization factor is given by $J = \sum_i \alpha_i\tau_i$. For a distribution of D-A distances the transforms are calculated numerically, using

$$N_\omega = \frac{1}{J}\int_{r=0}^\infty \frac{P(r)\omega\tau_{DA}^2}{1 + \omega^2\tau_{DA}^2} dr \tag{22}$$

$$D_\omega = \frac{1}{J}\int_{r=0}^\infty \frac{P(r)\tau_{DA}}{1 + \omega^2\tau_{DA}^2} dr \tag{23}$$

where the normalization factor J is given by

$$J = \left(\int_0^\infty P(r) \, dr\right)\left(\int_0^\infty I_{DA}(t) \, dt\right) \tag{24}$$

Depending upon $P(r)$ the integral from $r = 0$ to infinity may not be equal to unity. This integral will be less than unity when part of the distribution occurs below $r = 0$. The use of $\int_0^\infty P(r) \, dr$ in eq. 24 is equivalent to normalizing $P(r)$ to unity. For Förster kinetics with and without diffusion the transforms are also calculated numerically.

3. Materials and methods

The syntheses of the donor control (NMN) and donor-acceptor pair (NU2D) have been described previously [25,26]. The quantum yields of NMN were measured relative to a value of 0.13 for tryptophan in water at 20 °C [27]. These quantum yields and spectral properties of the donor and acceptor yielded R_0 values of 23.4–20.9 Å, depending upon temperature and/or solvent. Frequency-domain measurements were performed on the instrument described previously in detail [23]. The excitation source was a 3.79 MHz train of pulses, about 7 ps wide, obtained from the cavity-dumped output of a synchronously pumped rhodamine 6G dye laser. The light was frequency-doubled to 290 nm by a KDP crystal. The light

source is intrinsically modulated to many gigahertz and is used to excite the sample directly. The modulated emission was detected by using a microchannel plate photomultiplier tube (R1564U, Hamamatsu), which was externally cross-correlated. All intensity decays were measured by using rotation-free polarization conditions, with the donor emission selected by a 340 nm interference filter (10 nm bandwidth). For all analyses the uncertainties in the phase ($\delta\phi$) and modulation (δm) values were taken as 0.2° and 0.005, respectively. Sample temperatures were stabilized with accuracy ±1°C.

4. Results and discussion

4.1. Spectral properties

The donor and donor-acceptor pair used in this study are shown in scheme 1. The control molecule NMN contains only the naphthalene donor. The decay characteristics of the donor (NMN) are needed to determine the effects of the acceptor on the donor decay of NU2D, independent of the intrinsic decay of the donor.

Emission spectra of the donor NMN and of the D-A pair NU2D in propylene glycol are shown in fig. 1. The donor emission is due to the naphthalene moiety and is centered near 340 nm. The emission from the dansyl acceptor occurs near 510 nm. The donor emission is quenched by energy transfer at 0 and 80°C. At 80°C the energy transfer efficiency is significantly higher than at

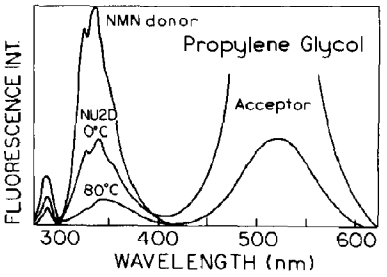

Fig. 1. Emission spectra of the NMN donor and NU2D donor-acceptor system.

0°C, which was expected as a result of increased end-to-end diffusion at the higher temperature.

4.2. Properties of solutions

Table 1 describes the relative viscosity and the expected effects of diffusion for the solutions used in this study. It should be noted that the differences were calculated for assumed radii of 5 Å for both the donor and acceptor molecules, and ignore the influence of the polymethylene chain on D-to-A diffusion. We calculated (eq. 1) the mean distance for diffusion during the lifetime of the excited state. This lifetime was calculated from the multiexponential parameters which describe the donor decay of NU2D. Based upon this analysis the mean distance the donor or acceptor can diffuse during the donor decay time increases from 3.4 to 16.2 Å as the temperature of propylene glycol is increased from 0 to 80°C. An alternative parameter is the relative mean diffusion distance

Table 1

Properties of solutions

Solvent	Temperature (°C)	η (cP)	D ($\times 10^{-7}$ cm^2/s)	$\bar{\tau}$ (ns)	$\Delta\bar{x}$ (Å)	$\Delta\bar{x}_{rel}$
PG	0	193	0.21 [a]	27.8 [c]	3.4	1
	20	48.3	0.88	20.2	6.0	1.76
	40	16.7	2.73	12.2	8.2	2.41
	60	5.8 [b]	8.38	7.7	11.4	3.35
	80	2.0 [b]	25.76	5.4	16.2	4.76
MeOH	20	0.6	71.30	2.0	17.0	5.00

[a] Calculated using eq. 1 with $R = 5$ Å.

[b] Obtained from extrapolation.

[c] The mean decay time of the donor decay of NU2D was calculated from the three-exponential analysis (table 2) using $\bar{\tau} = \Sigma\alpha_i\tau_i^2 = \Sigma f_i\tau_i$, where $f_i = \alpha_i\tau_i$ is the fractional intensity of the i-th component.

$\Delta\bar{x}_{rel} = \Delta\bar{x}/\Delta\bar{x}(0\,^{\circ}C)$, which is expected to increase 5-fold as the temperature and/or solvent is varied.

4.3. Multiexponential analysis

We analyzed the donor frequency responses for NMN and NU2D in terms of the multiexponential model (table 2). This is informative because one expects the D-to-A distance distribution to result in a complex donor decay, i.e., a distribution of distances results in increased deviations from the single-exponential model. This effect is clearly evident in fig. 2. The intensity decay of the donor alone (NMN) is essentially a single exponential at 0 °C (fig. 2) and at the other temperatures (table 2). This is seen from the close overlap of the frequency-domain data from NMN (●) with the best single-exponential fit (——).

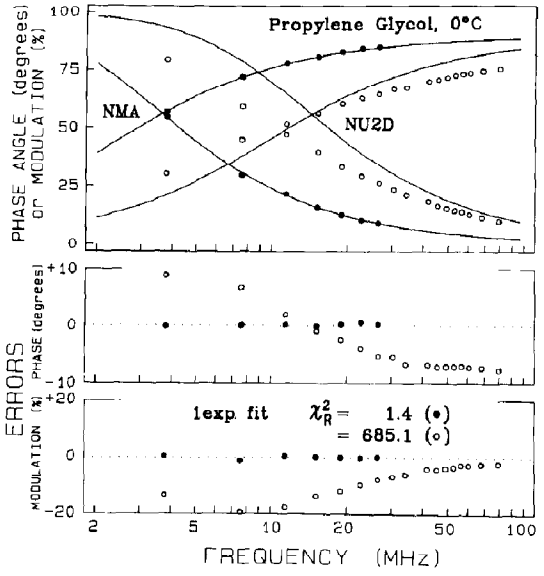

Fig. 2. Frequency response of the donor emission of NMN and NU2D donor-acceptor system.

Table 2

Multiexponential analysis of the intensity decays for NMN and NU2D

Solvent	Temperature (°C)	NMN (donor)		NU2D (D-A)			χ^2_R		
		τ (ns)	χ^2_R	$\bar{\tau}_i$ (ns)	α_i	f_i	1	2	3
PG	0	65.0	1.4	2.0 [a]	0.242	0.029			
				10.3	0.419	0.258			
				35.2	0.339	0.713	685.1	15.1	1.4
	20	58.3	1.4	2.8	0.274	0.060			
				10.1	0.428	0.335			
				26.0	0.298	0.605	461.1	6.1	1.4
	40	53.7	1.0	2.6	0.274	0.082			
				8.9	0.589	0.595			
				20.8	0.137	0.323	243.5	4.6	1.1
	60	47.3	0.8	1.9	0.289	0.099			
				5.9	0.609	0.641			
				14.2	0.102	0.260	208.7	4.9	1.9
	80	41.3	0.9	2.4	0.364	0.199			
				5.6	0.633	0.782			
				27.4	0.003	0.019	52.1	1.6	1.4
MeOH	20	24.4	1.2	0.4	0.037	0.009			
				1.5	0.670	0.549			
				2.7	0.293	0.442	27.9	1.1	0.9

[a] The listed amplitudes and decay times are for the three-exponential fits to the donor frequency response.

In contrast, the intensity decay of the naphthalene emission from NU2D is strongly heterogeneous (fig. 2) and can be fitted only with three-exponential decays. This heterogeneity is progressively decreased if the viscosity is lower, as can be seen from the decreasing values of χ_R^2 for the single-exponential fits (table 2). The triple-exponential parameters in table 2 can be regarded as representing the time-resolved decay, which can be compared with predictions of molecular dynamics simulations of this system. This effect is consistent with the predictions by Thomas et al. [28] for the so-called rapid diffusion limit, where the donor decay becomes a single exponential.

4.4. *Förster kinetics without diffusion*

We analyzed the data using the Förster equation (eq. 2), which does not include the possibility of diffusion. We reasoned that this nondiffusional model should provide a modest fit to the data at low temperatures where the viscosity is high, and that the fit should become increasingly poorer at higher temperatures. This trend was found, as can be seen from the increasing values of χ_R^2 for the higher temperatures (table 3). The good fit at low temperature indicates that our use of the multiacceptor theory (Förster eq. 2) for our single acceptor molecule is a reasonable approximation. Representative low- and high-temperature frequency responses are shown in fig. 3. At 0 °C, where diffusion is minimal, eq. 2 provides a good approximation to the measured frequency response (●). At 80 °C the data (○) are not even approximated by the Förster equation. It should be noted that the high-temperature frequency response is compressed along the frequency axis, as compared to the best-fit Förster curve. This indicates that end-to-end diffusion results in a donor decay which is more like a single exponential that can be obtained from eq. 2. The apparent concentrations C_A recovered from eq. 2 progressively increase with diffusion (table 3). These data and analysis demonstrate that end-to-end diffusion is easily detected from the frequency response of the donor.

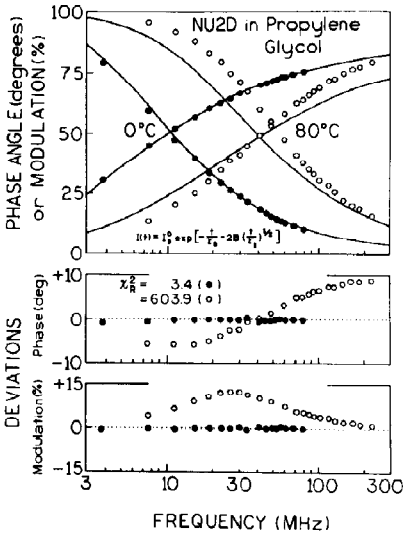

Fig. 3. Fits to Förster kinetics without diffusion (eq. 2) in the case of high and low viscosity (0 and 80 °C).

4.5. *Förster kinetics with diffusion*

The frequency-domain data were analyzed in terms of diffusion-dependent energy transfer,

Table 3

Förster kinetics without diffusion analysis

Solvent	Temperature (°C)	R_0 (Å)	C_A ($\times 10^{-2}$) (M)	C_A' ($\times 10^{-2}$) (M)	χ_R^2
PG	0	23.42 [a]	3.7 [b]	3.8 [c]	3.4
	20	23.00	4.5	5.2	26.7
	40	22.64	6.1	7.2	171.4
	60	22.17	8.5	9.4	254.1
	80	21.62	9.7	10.9	603.9
MeOH	20	20.90	14.3	15.2	693.1

[a] Calculated from emission of donor and absorption of acceptor according to eq. 4.
[b] Apparent concentration calculated from eq. 2.
[c] Effective acceptor concentrations calculated from the distance distributions (table 5) and eqs 25–27.

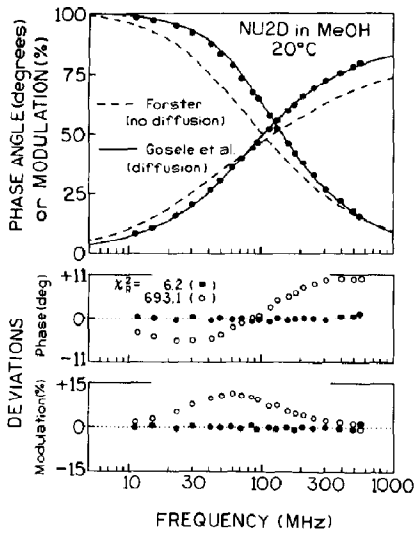

Fig. 4. Frequency response of NU2D donor-acceptor emission in methanol and fits to Förster kinetics with (———, ●) and without diffusion (- - - - -, ○).

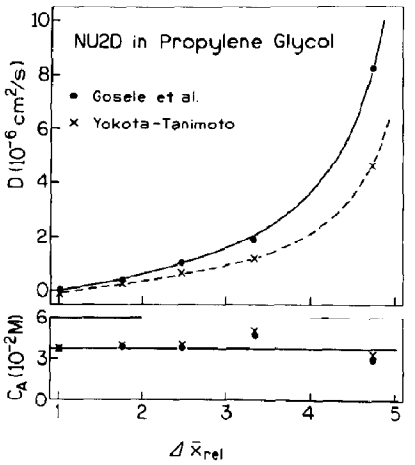

Fig. 5. Dependence of C_A and D (recovered from models of Yokota and Tanimoto and Gosele et al.) with the relative diffusion and distance in the solution (represented by $\Delta\bar{x}_{rel}$).

according to eqs 5–8 for the models of Yokota and Tanimoto and Gosele et al. (table 4). The data for NU2D in methanol (fig. 4) cannot be fitted using the Förster equations (- - -, ○; $\chi^2_R = 693$), but are well fitted using the model of Gosele et al. (———, ○; $\chi^2_R = 6.2$). In general, these models provide an improved and acceptable fit to the data in all cases where end-to-end diffusion contributes to the energy-transfer process. The recovered acceptor concentrations (C_A) are relatively stable (especially in the model of Gosele et al.) and the diffusion coefficients appear to be reasonable (fig. 5). For instance, at 20 and 80 °C, a 5 Å sphere is expected to have diffusion coefficients near 0.09×10^{-6} and 2.58×10^{-6} cm^2/s, respectively (eq. 1). The observed values are about 2-fold higher, 0.14 and 4.59×10^{-6} cm^2/s, which is probably due to the fact that both D and A are diffusing, and the apparent value of D is the sum of both their diffusion coefficients. The 100-fold improvement

Table 4

Diffusion-dependent energy-transfer analysis

Solvent	Temperature (°C)	Yokoto-Tanimoto			Gosele et al.		
		C_A ($\times 10^{-2}$) (M)	D ($\times 10^{-6}$) (cm^2/s)	χ^2_R	C_A ($\times 10^{-2}$) (M)	D ($\times 10^{-6}$) (cm^2/s)	χ^2_R
PG	0	3.7	$0.5 \cdot 10^{-4}$	3.7	3.7	$0.4 \cdot 10^{-4}$	3.5
	20	4.0	0.14	5.8	3.9	0.16	5.4
		⟨3.7⟩ [a]	0.24	11.0	⟨3.7⟩	0.26	8.5
	40	4.1	0.67	11.8	3.8	0.98	9.8
		⟨3.7⟩	0.92	16.1	⟨3.7⟩	1.12	10.1
	60	5.1	1.14	15.4	4.7	1.93	13.4
		⟨3.7⟩	2.46	41.7	⟨3.7⟩	3.25	26.8
	80	3.3	4.59	8.2	2.9	8.13	7.9
		⟨3.7⟩	3.77	9.2	⟨3.7⟩	5.10	14.2
MeOH	20	3.8	13.6	6.3	3.2	29.99	6.2
		⟨3.7⟩	14.0	6.2	⟨3.7⟩	19.78	6.8

[a] ⟨⟩ indicate fixed parameter.

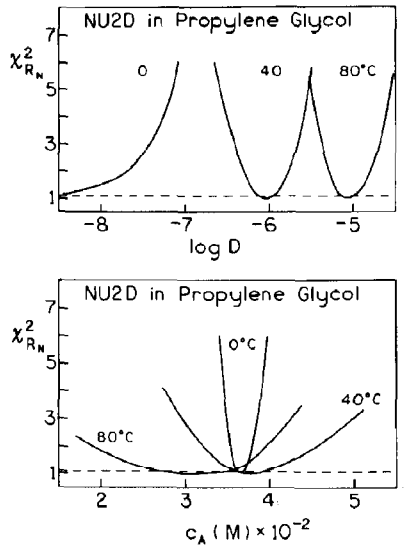

Fig. 6. χ^2_R surfaces for D (top, D in cm^2/s) and C_A (bottom) recovered from model of Gosele et al.

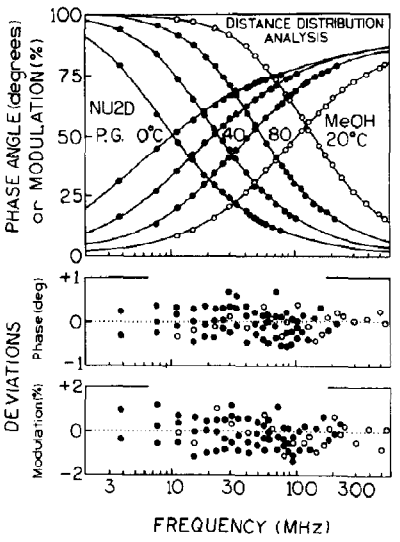

Fig. 7. Distance distribution analysis for NU2D.

in goodness-of-fit, as compared with the model without diffusion, indicates that these models can describe the time-dependent decays of D-A pairs with end-to-end diffusion.

It is thought to be difficult to recover the end-to-end diffusion coefficients due to correlations between the parameters [19]. The ability to resolve both parameters, C_A and D, from the model of Gosele et al. is shown in fig. 6, which shows the dependence of χ^2_R on the values of C_A and D. To construct these χ^2_R surfaces, we held one parameter constant at the value indicated by the x-axis, and the other parameter was allowed to vary to provide the best fit to the data. The steepness of these surfaces suggests that the frequency-domain measurements can provide useful data for studies of intramolecular dynamics.

4.6. Distance distribution analysis

We also analyzed the frequency-domain data in terms of static (no diffusion) distance distributions. Surprisingly, we obtained excellent fits not only for solutions with high viscosity, but also for the fluid solutions (table 5 and fig. 7). The influence of diffusion on energy transfer is visible from the changes in the mean distance and in the shape of the Gaussian profiles, which become sharper as diffusion increases. The apparent distribution profiles are shown in fig. 8, where the inset shows the dependence of the center of the distri-

Table 5

Distance distribution analysis for NU2D

Solvent	Temperature (°C)	R_0 (Å)	$\bar{r}$ (Å)	hw (Å)	χ^2_R
PG	0	23.42	18.0	12.4	1.1
	20	23.00	17.7	8.5	1.4
	40	22.64	16.8	5.5	1.4
	60	22.17	15.5	4.4	2.0
	80	21.62	15.1	2.7	1.4
MeOH	20	20.9	13.6	2.0	0.9

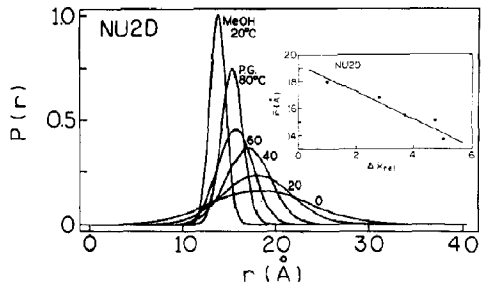

Fig. 8. Distance distribution profiles for NU2D. (inset) Dependence of $\bar{r}$ upon the properties of solutions (represented by $\Delta\bar{x}_{rel}$).

bution on the relative mean diffusion distance $\Delta\bar{x}_{rel}$. A similar dependence has been found for the half-width of the distribution (not shown). As expected, the apparent distribution parameters are correlated with the molecular diffusion parameter $\Delta\bar{x}$.

The apparent distance distributions recovered from this analysis allow us to calculate the effective concentration of acceptor around the donor. The single acceptor is assumed to be distributed in an effective volume ($\bar{v}$), which is determined by

$$\bar{v} = \frac{\int vP(v)\,dv}{\int P(v)\,dv} \tag{25}$$

Recalling that $v = 4\pi r^3/3$ and $dv = 4\pi r^2\,dr$ one obtains

$$\bar{v} = \frac{4}{3}\pi \frac{\int r^5 P(r)\,dr}{\int r^2 P(r)\,dr} \tag{26}$$

The effective concentration of the acceptor (C_A') is thus

$$C_A' = 1/\bar{v}N' \tag{27}$$

where N' is Avogadro's number in molecules per millimole. The acceptor concentrations calculated in this manner are summarized in table 3. These concentrations (C_A) are in good agreement with those calculated from the Förster equation without diffusion, indicating that an increase in the apparent acceptor concentration can partially account for the effects of diffusion.

The calculated acceptor concentration from the low-temperature data is not influenced by diffusion, and should therefore be the correct concentration at all temperatures. In fact, the acceptor concentrations recovered from the diffusional models were all close to this value (table 4). Additionally, the acceptor concentration could be held fixed at this value with only modest effects in the goodness-of-fit (table 3).

5. Conclusions

Frequency-domain measurements of a D-A pair revealed the effects of end-to-end diffusion on the donor decay law. The data were analyzed in terms of models which are rigorously correct for multiple randomly distributed acceptors. Consequently, the recovered parameters are apparent. Nonetheless, these parameters clearly reveal the effects of end-to-end diffusion, as seen by increased apparent concentrations for the Förster model, increased diffusion coefficients for the models of Yokota and Tanimoto and Gosele et al., and compressed apparent distance distributions. The high apparent resolution of these apparent parameters suggests the frequency-domain data will be useful in studies of intramolecular molecular dynamics.

Acknowledgements

This work supported by grants DMB-8804913 and DMB-8502835 from the National Science Foundation, and grants GM-35154 and GM39617 from the National Institutes of Health. J.R.L. and W.W. acknowledge support from the Medical Biotechnology Center at the University of Maryland.

References

1 L. Stryer and R.P. Haugland, Proc. Natl. Acad. Sci. U.S.A. 58 (1967) 719.
2 G. Weber and F.W.J. Tale, Trans. Faraday Soc. 54 (1958) 640.

3 J.R. Lakowicz, M.L. Johnson, W. Wiczk, A. Bhat and R.F. Steiner, Chem. Phys. Lett. 138 (1987) 587.
4 B. Valeur, in: Fluorescent biomolecules, eds D.M. Jameson and G.D. Reinhart (Plenum, New York, 1989) p. 269.
5 I.Z. Steinberg, Annu. Rev. Biochem. 40 (1971) 83.
6 L. Stryer, Annu. Rev. Biochem. 47 (1978) 819.
7 H.C. Cheung, C.K. Wang and F. Garland, Biochemistry 21 (1982) 5135.
8 J.R. Lakowicz, Principles of fluorescence spectroscopy (Plenum, New York, 1983) ch. 10, p. 303.
9 J.R. Lakowicz, I. Gryczynski, H.C. Cheung, C.K. Wang and M.L. Johnson, Biopolymers 27 (1988) 821.
10 J.R. Lakowicz, I. Gryczynski, H.C. Cheung, C.K. Wang, M.L. Johnson and N. Joshi, Biochemistry 27 (1988) 9149.
11 Yu Kurskii and A.S. Selivanenko, Opt. Spectrosc. 8 (1960) 340.
12 K.S. Bagdasaryan and A.L. Muller, Opt. Spectrosc. 18 (1965) 558.
13 J. Feitelson, J. Chem. Phys. 44 (1966) 1497.
14 R. Voltz, G. Laustriat and A. Coche, J. Chim. Phys. 63 (1966) 1253.
15 M. Yokota and O. Tanimoto, J. Phys. Soc. Jap. 22 (1967) 779.
16 U. Gosele, M. Hauser, U.K.A. Klein and R. Frey, Chem. Phys. Lett. 37 (1975) 519.
17 E. Haas, E. Katchalski-Katzir and I.Z. Steinberg, Biopolymers 17 (1978) 11.
18 E. Haas and I.Z. Steinberg, Biophys. J. 46 (1984) 429.
19 J.M. Beechem and E. Haas, Biophys. J. 49 (1989) 1225.
20 T. Förster, Ann. Phys. (Leipzig) 2 (1948) 55.
21 J.R. Lakowicz, G. Laczko, I. Gryczynski, H. Szmacinski, W. Wiczk and M.L. Johnson, Ber. Bunsenges. Phys. Chem. 93 (1989) 316.
22 J.R. Lakowicz and B.P. Maliwal, Biophys. Chem. 21 (1985) 61.
23 J.R. Lakowicz, G. Laczko and I. Gryczynski, Rev. Sci. Instrum. 57 (1986) 2499.
24 J.R. Lakowicz, G. Laczko, H. Cherek, E. Gratton and M. Limkeman, Biophys. J. 46 (1984) 463.
25 I. Gryczynski, W. Wiczk, M.L. Johnson and J.R. Lakowicz, Chem. Phys. Lett. 145 (1988) 439.
26 J.R. Lakowicz, W. Wiczk, I. Gryczynski and M. Fishman, manuscript in preparation.
27 R.F. Chen, Anal. Lett. 1 (1967) 35.
28 D. Thomas, W.F. Carlsen and L. Stryer, Proc. Natl. Acad. Sci. U.S.A. 75 (1978) 5746.